Corticotropin releasing factor alters the functional diversity of accumbal cholinergic interneurons

Anna E. Ingebretson[1,2] and Julia C. Lemos[1,2]

Affiliations

1. Department of Neuroscience, University of Minnesota-Twin Cities, Minneapolis, MN.
2. Medical Discovery Team on Addiction, University of Minnesota, Minneapolis, MN.

*Corresponding author: Dr. Julia C. Lemos
jlemos@umn.edu
321 Church Street
Minneapolis, MN 55406

Running Title: Cholinergic functional diversity in the NAc shell

Keywords: nucleus accumbens, cholinergic interneuron, corticotropin releasing factor

Number of pages: 29

Number of figures: 5

Word count: 8851

Abstract: 242

Acknowledgements: This study was funded by K99/R00 Pathway to Independence award (MH109627) to JCL and NIMH BRAINS R01 (MH122749). We thank Drs. David Lovinger, Veronica Alvarez, and Erin Calipari for their useful input. Dr. Kavya Devarakonda contributed key edits to the manuscript. The authors declare no competing financial interests.

Abstract

Cholinergic interneurons (ChIs) provide the main source of acetylcholine in the striatum and have emerged as a critical modulator of behavioral flexibility, motivation, and associative learning. In the dorsal striatum, ChIs display heterogeneous firing patterns. Here, we investigated the spontaneous firing patterns of ChIs in the nucleus accumbens (NAc) shell, a region of the ventral striatum. Using male and female mice, we performed cell-attached patch clamp electrophysiology recordings from ChIs. We identified four distinct ChI firing signatures: regular single-spiking, irregular single-spiking, rhythmic bursting followed by pauses or low activity, and a mixed-mode pattern composed of bursting activity and regular single spiking. ChIs from females had lower firing rates compared to males and had both a higher proportion of mixed-mode firing patterns and a lower proportion of regular single-spiking neurons compared to males. We further observed that across the estrous cycle, the estrus phase was characterized by higher proportions of mixed-mode, rhythmic bursting, and irregular ChI firing patterns compared to other phases. ChI firing mode was not driven by glutamatergic synaptic transmission in the slice preparation. Using pooled data from males and females, we examined the how the stress-associated neuropeptide corticotropin releasing factor (CRF) impacts these firing patterns. ChI firing patterns showed differential sensitivity to CRF. Furthermore, CRF shifted the proportion of ChI firing patterns toward more regular spiking activity over bursting patterns. These findings highlight the heterogeneous nature of ChI firing patterns, which may have implications for accumbal-dependent motivated behaviors.

New and Noteworthy: ChIs within the dorsal and ventral striatum can exert a huge influence on network output and motivated behaviors. However, the firing patterns and neuromodulation of ChIs within the ventral striatum,specifically the NAc shell, are understudied. Here we report that NAc shell ChIs have a heterogenous distribution of ChI firing patterns that are labile and can be modulated by the stress-linked neuropeptide CRF and by estrous cycle.

Introduction

Cholinergic interneurons (ChIs) provide the main source of acetylcholine modulation of striatal circuit function (Gonzales and Smith, 2015). ChIs make up approximately 1-2% of all the neurons within the dorsal and ventral striatum (Bolam, Wainer and Smith, 1984; Bonsi et al., 2011; Nosaka and Wickens, 2022). However, these large aspiny neurons are highly ramified such that this relatively small number of neurons can serve as a master regulator of striatal output (Gonzales and Smith, 2015; Nosaka and Wickens, 2022). A central functional property of this population of neurons is that they are spontaneously active both in in vivo and ex vivo preparations (Gonzales and Smith, 2015). In the dorsal striatum, ChIs display heterogeneous firing patterns. Bennett and Wilson (1999) identified three categories of spontaneously firing ChIs within the dorsal striatum. “Regular,” “irregular,” and “rhythmic bursting” signatures could be distinguished by their differential firing rates and coefficients of variation of the inter-event interval (IEI) distribution (Bennett and Wilson, 1999). “Regular” ChIs had high firing rates distinguished by regularly occurring single spikes that had narrow, unimodal IEI distributions and low IEI CVs, characteristic of canonical pacemaker firing. “Irregular” ChIs had lower firing rates and higher CVs, indicating greater variability in spike timing. Finally, “rhythmic bursting” ChIs were characterized by a rhythmic firing pattern consisting of bursts of spikes interspersed with pauses in firing activity that yielded a skewed or bimodal IEI distribution with shorter intraburst intervals comprising the mean interval and longer interburst pauses forming the tail of the distribution; this high degree of temporal variability produced low overall firing rates and very high IEI CVs (Bennett, Callaway and Wilson, 2000; Bennett and Wilson, 1999). Bennet and Wilson went on to demonstrate that these disparate firing properties were not driven by excitatory or inhibitory synaptic transmission, but by differential intrinsic properties. Specifically, the small calcium-activated potassium channel (SK) was identified as a key regulator of firing properties (Bennett, Callaway and Wilson, 2000; Bennett and Wilson, 1999; Goldberg and Wilson, 2005; Wilson, 2005).

The firing properties of different cell types within the NAc core and shell, including ChIs, remain largely unexplored. It is unknown whether the functional heterogeneity of ChIs in the dorsal striatum is also present in the ventral striatum. While

early studies included both male and female animals, sex and sex hormones as biological variables of interest were not explored. In addition, the functional relevance of this complex spiking behavior has not been fully examined. Understanding the cellular properties of NAc shell ChIs may provide important mechanistic insights into their role in motivated behavior.

Recent work has renewed interest in the cellular properties of ChIs and how heterogeneous firing modes might relate to the functional role of ChIs in motivated behavior. For example, shifts from tonic ChI pacemaker activity to a burst-pause mode in the dorsal striatum has been suggested to encode a salient environmental stimulus that generates an attentional and, perhaps, a motivational shift (Ding et al., 2010; Krok et al., 2023; Nosaka and Wickens, 2022; Zhang and Cragg, 2017; Zucca et al., 2018). To our knowledge, no in vivo electrophysiology studies have been carried out focusing on ChIs in the NAc. However, both bursts and ramps of ChI population activity are correlated with motivated approach behavior (Mohebi, Collins and Berke, 2023). Furthermore, ChI population activity within the NAc shell both tracks with and promotes reward learning (Al-Hasani et al., 2021). While a mechanistic understanding of how these salient environmental stimuli are translated into molecular and cellular signals in the NAc is still unclear, one potential mechanism is through the release of neuropeptides.

Corticotropin-releasing factor (CRF) is a stress-associated neuropeptide that is widely distributed and released in the brain and the periphery during periods of high arousal and salience, including novelty (Bale and Vale, 2004; Dabrowska et al., 2013; Henckens, Deussing and Chen, 2016; Lemos et al., 2012). In the cortex, CRF is released in response to anticipatory cues that signal food delivery (Merali, McIntosh and Anisman, 2004). In the NAc, CRF is released in response to novelty and facilitates novelty exploration (Lemos et al., 2012). Exogenous application of CRF in the NAc can promote appetitive behaviors and potentiate both dopamine and acetylcholine transmission (Chen et al., 2012; Lemos et al., 2012; Lim et al., 2007; Pecina, Schulkin and Berridge, 2006). Finally, CRF potentiates ChI firing rate in the NAc core and dorsal striatum via activation of CRF type 1 receptors (CRF-R1), cAMP, and SK channel

activation in male mice (Lemos, Shin and Alvarez, 2019). Given the role for striatal ChIs in encoding salient stimuli, CRF might shape salience encoding in the NAc via modulation of ChI firing patterns.In this study, we investigated the diversity of spontaneous firing properties in the NAc shell of both male and female mice and across the estrous cycle in female mice. We had previously not characterized ChI firing patterns or CRF effects in the NAc shell. We examined if ChIs with different spontaneous firing properties differentially respond to CRF application at different concentrations. During this investigation, we found that there were four distinct categories of ChI based on temporal firing patterns. We also found interesting sex differences and sensitivity to CRF based on this categorization. Importantly, we found that CRF shifts the distribution of firing modes toward a more regular tonic firing pattern as opposed to a more rhythmic or bursting mode. These data may provide a cellular mechanism for how salient stimuli shift the circuit level output of the NAc to facilitate appropriate behavioral responses to the environment.

Methods and Material

All procedures were performed in accordance with guidelines from the Institutional Animal Care and Use Committee at the University of Minnesota.

Animals: Male and female mice (post-natal day 60-180) were group housed and kept under a 12h-light cycle (6:30 ON/18:30 OFF) with food and water available *ad libitum*. For all *ex vivo* electrophysiology experiments, ChAT-IRES-Cre$^{+/-}$ mice (B6N.129S6(B6)-Chattm2(cre)Lowl/J, Jackson Laboratory stock number 018957) crossed with Ai14;tdTomato reporter mice (B6.Cg-Gt(ROSA)26Sortm14(CAG-tdTomato)Hze/J, Jackson Laboratory stock number 007914) were used to easily visualize ChIs.

Estrous cycle tracking: Vaginal lavage methods were used to track the estrous cycle of female mice over a 8–10 day period in order to capture two full cycles. Briefly, 20 µl of sterile saline was rapidly pipetted in and out of the vagina such that vaginal cells would be collected within the solution. The sample was dried, stained with cresyl violet, and assessed under the microscope. Based on the proportion of leukocytes, cornified

epithelial cells and nucleated epithelial cells, as well as the size of the vaginal opening, we classified females as in proestrus, estrus, metestrus or diestrus (Cora, Kooistra and Travlos, 2015).

Ex vivo electrophysiology: Coronal brain slices (240 µm) containing the NAc core and shell were prepared from 8–24-week-old *ChAT-ires-CRE*$^{+/-}$*;Ai14 tdTomato* mice. Slices were cut in ice-cold cutting solution (in mM): 225 sucrose, 13.9 NaCl, 26.2 $NaHCO_3$, 1 NaH_2PO_4, 1.25 glucose, 2.5 KCl, 0.1 $CaCl_2$, 4.9 $MgCl_2$ and 3 kynurenic acid. Slices were maintained in oxygenated artificial cerebrospinal fluid (ACSF) containing (in mM): 124 NaCl, 2.5 KCl, 2.5 $CaCl_2$, 1.3 $MgCl_2$, 26.2 $NaHCO_3$, 1 NaH_2PO_4 and 20 glucose (~310–315 mOsm) at room temperature following a 1hr recovery period at 33ºC. Cell-attached recordings were made in voltage clamp mode at 30-33ºC to assess firing properties and to measure the effect of CRF on ChI firing frequency without causing "run-down" due to dialyzing the cell with internal solution in a whole-cell configuration. For cell-attached recordings, electrodes were filled with filtered ACSF identical to the external solution. A gigaohm seal was achieved, maintained, and monitored. Cells in which the gigaohm seal had degraded were excluded. Data were acquired at 5 kHz and filtered at 1 kHz using either a SutterPatch or Multiclamp 700B (Molecular Devices). Data was analyzed using Igor or pClamp (Clampfit, v. 10.3).

Drug Application: 2,3-Dioxo-6-nitro-1,2,3,4-tetrahydrobenzo[*f*]quinoxaline-7-sulfonamide (NBQX), 3-((*R*)-2-Carboxypiperazin-4-yl)-propyl-1-phosphonic acid (R-CPP), and rat/human CRF were acquired from R & D systems (Tocris) and bath applied to the slice preparation. NBQX and CPP were both applied at a final concentration of 5 µM. CRF was bath applied at concentrations of 0, 3, 10, 100 nM. These concentrations of CRF were based on our previous work (Lemos et al., 2019), where we applied CRF to NAc core slices from males and found that the EC50 was 8.6 nM and the maximal concentration was 100 nM.

Statistics: Statistical analysis was performed in Prism (GraphPad) and Excel on spiking data extracted from the SutterPatch or Multiclamp 700B platforms. For each cell with a baseline firing rate greater than 0.5 Hz, analysis was performed on three minutes of stable, continuous recording following a five-minute equilibration period. Cells with firing

rates less than 0.5 Hz were discarded. The mean firing rate for each cell was calculated as the mean number of spikes per second for the analysis recording section. To calculate the coefficient of variation (CV) of spiking activity for each cell, the inter-event interval histogram was extracted from the analysis recording section, and both the mean and the standard deviation was calculated. The CV was then calculated as the standard deviation divided by the mean IEI. For grouped data, a Kolmogorov-Smirnov test was used to test normality. If one or more groups failed normality, non-parametric analyses were chosen. Two-tailed paired t-tests, one-way ANOVAs, or one-tailed t-tests were used when appropriate and stated. For analysis of changes in cell proportions, a Chi-squared test was used with numbers that were rounded to the nearest whole integer. All data are presented as mean ± SEM. Results were considered significant at an alpha of 0.05.

Results

NAc shell ChIs have four distinct firing modes

We sampled a total of 108 ChIs (Cre+) from male and female *ChAT-ires-CRE*$^{+/-}$*;Ai14 tdTomato* mice. Bennett and Wilson (1999) categorized ChI spontaneous firing into three categories: “regular,” “irregular,” and “rhythmic bursting.” Based on Bennet and Wilson’s observations and classification approach, we classified cells using both visual inspection and the coefficient of variation (CV) of each cell’s mean inter-event interval (IEI), which provides a measure of each cell’s spike timing variability. Quantification of the firing rate and IEI CV validated our ChI sorting approach. Cells with regular, single-spiking firing modes and narrow IEI distributions tended to have low CVs of 0.25 or less. Irregular cells were characterized by irregularly-occurring single spikes, wider IEI distributions, and typically had CV values of 0.30 - 0.65. Rhythmic bursting cells displayed high-frequency bursts of activity followed either by complete pauses in activity or occasional single spikes; these cells usually had skewed or bimodal IEI distributions and the highest CV values typically of 0.70 - 1.00. However, we also observed another type that seemed to display a mixture of these types, characterized by a robust, regular firing pattern with intermittent burst-like firing and a variable CV (0.30 - 0.80), depending on the proportion of burst motifs to regular single spiking. This cell type was

distinguished from the other three as “mixed mode” ChIs. Figure 1a,b show example traces and corresponding frequency histograms of these four different ChI firing patterns. We first assessed the proportions of all ChIs based on the classifiers used by Bennett and Wilson along with our own visual classification. We found that 45% of NAc shell ChIs displayed an irregular firing pattern, 26% had a regular firing pattern, 11% had a rhythmic bursting firing pattern and 19% had a mixed mode firing pattern (Figure 1c). Under our classification system, regular ChIs had higher firing rates than rhythmic or irregular ChIs. The newly identified mixed mode ChI firing pattern had a significantly higher firing rate than the irregular ChIs (regular: 3.9± 0.4 Hz; rhythmic: 2.2 ± 0.2 Hz; irregular: 1.9± 0.1 Hz; mixed mode: 3.2± 0.2 Hz, one-way ANOVA, $F_{3,104} = 14.96$, $p < 0.0001$, $n = 108$, see Figure 1d for Tukey’s post-hoc t-tests). When we analyzed the CV of the IEI, regular ChIs had significantly lower CVs compared to rhythmic or irregular firing patterns. Mixed mode ChIs had a significantly higher CV compared to regular ChIs (regular: 0.28± 0.01; rhythmic: 0.89 ± 0.07; irregular: 0.50± 0.02; mixed mode: 0.49± 0.04, Kruskal-Wallis test, $F_{3,104} = 44.18$, $p < 0.0001$, $n = 108$, see Figure 1e for Dunn’s post-hoc comparison).Thus, mixed mode neurons can be distinguished from regular and irregular patterns by their higher firing rates than irregular neurons and higher CVs compared to regular neurons. Similar to Bennett and Wilson (1999), there was a significant negative correlation between the firing rate and the IEI CV ($r = -0.464$, $p < 0.0001$), indicating that higher firing rates were associated with lower spike timing variability.

Sex differences in the basal functional properties of NAc shell ChIs

To our knowledge, sex-dependent differences in ChI properties have not been assessed. We analyzed differences in firing rates, IEI CVs, and firing mode proportions between male and female mice, and in females across the estrous cycle. On average, males had significantly higher firing rates than females (male: 3.6± 0.4 Hz, $n = 26$; female 2.5 ± 0.2 Hz, $n = 79$, Mann-Whitney test, $p =0.0024$, Figure 2a,b). As described in the methods, we tracked the female estrous cycle over an 8–10-day period to be confident of estrous cycle stage on the day of sacrifice. A final vaginal lavage was done

prior to sacrifice, and the cycle stage was visualized and noted (Figure 2d). While firing rates in females appeared lower than males across the estrous cycle, this was only significant in diestrus and estrus females when the female data was parsed (male: 3.6± 0.4 Hz, n = 26; female-proestrus: 2.6 ± 0.5 Hz, n = 14; female-estrus: 2.1 ± 0.2 Hz, n = 23; female-metestrus: 2.5 ± 0.3 Hz, n = 20, female-diestrus: 2.4 ± 0.5 Hz, n = 19, Kruskal-Wallis test, p = 0.0196, Dunnett's comparison test, male vs. female-estrus, p = 0.0169, male vs. female-diestrus, p = 0.0143, Figure 2e). Notably, the variance across groups for both firing rates and CVs were significantly different (Bartlett's test, p = 0.0112). There was trend for females to have a higher CV compared to males; however, this was not significant (Male: 0.43 ± 0.04, n = 26; Female 0.50± 0.03, n = 78, Mann-Whitney, p =0.0869, Figure 2c). Likewise, when comparing the CV of male and females across the estrous cycle, no significant differences were found (Kruskal-Wallis test, p = 0.2525). We next sorted our previously classified cells by sex and by estrous cycle. Interestingly, we found a significant difference in the proportion of ChI firing modes between males and females, driven by a higher proportional of "mixed mode" neurons and a lower proportion of "regular" neurons in female mice (Chi-square test, p = 0.0260, Figure 2g). There were also robust differences in cell type proportions across the estrous cycle (Chi-square test, p < 0.0001, Figure 2g). Notably, ChIs collected in the estrus phase had higher proportions of mixed mode, irregular, and rhythmic bursting firing patterns with very low proportions of regular firing patterns, compared to ChIs collected in other cycle stages. Taken together, the data demonstrate differences in ChI firing rates and patterns between males and females.

Effect of glutamatergic synaptic transmission on ChI spontaneous firing patterns

In the original analysis by Bennett and Wilson (1999), they demonstrated that the heterogeneous ChI firing patterns were not driven by glutamatergic synaptic transmission. To confirm that this was also true for the NAc shell, we recorded from ChIs in the presence of antagonists for AMPA (NBQX, 5 μM) and NMDA (CPP, 5 μM) in male and female mice. The total proportions of regular, rhythmic, irregular, and mixed mode ChIs was remarkably preserved in the presence of glutamatergic synaptic

blockers, even with a much smaller sample size (Chi-squared test, p = 0.6519, Figure 3a). There were no significant differences in the firing rate or CV in ChIs recorded in standard ACSF versus with the inclusion of AMPA and NMDA antagonists (control (n = 108) vs. NBQX/CPP (n = 14) - firing rate: 2.7± 0.2 Hz vs. 2.6 ± 0.4 Hz, Mann-Whitney test, p = 0.7947; CV: 0.48 ± 0.02 vs. 0.52 ± 0.07, Mann-Whitney test, p = 0.6633, Figure 3b,c). Finally, though not statistically significant, there was a qualitatively similar negative correlation between firing rate and CV as seen in control ACSF (r = -0.463, p = 0.096). These data are consistent with previous findings in the dorsal striatum that spontaneous firing patterns are not driven by glutamatergic synaptic transmission.

Differential CRF sensitivity based on ChI spontaneous firing pattern

CRF is released in the NAc in response to salient stimuli and potentiates ChI firing via sK channels (Lemos, Shin and Alvarez, 2019; Lemos et al., 2012). Given the importance of SK channels in determining dorsal striatal ChI firing properties (Bennett, Callaway and Wilson, 2000; Bennett and Wilson, 1999), we speculated that this may be a reasonable molecular candidate for how salient stimuli alter the firing properties of ChIs in the NAc. We assessed the ability of CRF to alter the firing rate, CV, and overall firing pattern of NAc shell ChIs collected from male and female mice, segregated into the four classifications based on their baseline firing patterns. We chose concentrations based on previous work done in the NAc core (Lemos, Shin and Alvarez, 2019). At the maximal concentration (100 nM), CRF significantly increased the firing rate of all four categories of ChI firing patterns (one-sample t-tests compared to 100% baseline, n = 6-17, Figure 4a,b,e,f,i,j,m,n). However, for 3 nM and 10 nM CRF, the responses varied depending on the basal spontaneous firing pattern of ChIs. CRF (10 nM) increased the firing rate above baseline significantly for regular, irregular, and mixed mode ChIs but not for rhythmic ChIs (one-sample t-tests compared to 100% baseline, n = 2-15, Figure 4b,f,j,n). CRF (3 nM) only increased the firing rate above baseline significantly for irregular ChIs (one-sample t-tests compared to 100% baseline, n = 2-9, Figure 4b,f,j,n). CRF (10, 100 nM) significantly reduced the IEI CV in irregular ChIs only, with no significant effect on regular, rhythmic, or mixed mode ChIs (one-sample t-tests compared to 0, n = 2-17, Figure 4c,g,k,o). Figure 4d,h,l,p indicate changes in the firing

pattern for each ChI classification following bath application of CRF (0,3,10, 100 nM). All ChI firing mode types displayed some pattern redistribution following drug application. However, regular ChI neurons were qualitatively the least impacted in terms of a shift in the spontaneous firing pattern.

We next directly compared the change in firing rate induced by 3 and 100 nM CRF based on firing pattern (the low and high end of our concentration response curve). There was a significant difference between irregular and mixed mode ChIs in CRF's ability to potentiate the firing rate at the lower concentration (one-way ANOVA, $F_{2,14}$ = 4.079, p = 0.0402; Tukey's multiple comparison test, irregular vs. mixed mode, p = 0.0468, n = 2-9, Figure 5a). In contrast, at the maximal concentration, CRF similarly potentiated ChI firing rate regardless of the basal spontaneous firing pattern (one-way ANOVA, $F_{3,35}$ = 1.058, p = 0.3793, n = 6-17, Figure 5b). We subsequently compared irregular and mixed mode ChIs across all three CRF concentrations using a two-way ANOVA and found a main effect of cell type but no significant interaction (two-way ANOVA, main effect of cell type, $F_{1.54}$ = 5.845, p = 0.0190, n = 4-17). We had previously shown that there was a negative correlation between CRF response and baseline firing rate (Lemos, Shin and Alvarez, 2019). We replicated this finding, demonstrating that the CRF response (percent of baseline firing) is negatively correlated with the baseline firing rate, best fit with a semi-log line (r^2 = -0.60, p < 0.001, Figure 5c). Finally, we assessed the firing patterns prior to and following CRF application (100 nM). Like the ChI firing pattern distribution assessed from all 108 cells, at baseline, the ChIs pre-CRF (100 nM) were composed of 24% regular, 9% rhythmic, 50% irregular and 17% mixed mode patterns. Following CRF (100 nM), this proportion was shifted to 42% regular, 5% rhythmic, 30% irregular and 23% mixed mode (Chi-squared test, p = 0.0075, n = 39, Figure 5d).

Discussion

In this study, we characterize the spontaneous firing properties of ChIs within the NAc shell of male and female mice. Previous foundational work described three modes of spontaneous firing patterns in dorsal striatal ChIs in 3–4-week-old rats: regular, rhythmic

bursting, and irregular (Bennett and Wilson, 1999). Here, we have extended this work to demonstrate that these patterns are conserved across species, sex, striatal regions and well into adulthood using an ex vivo slice preparation. However, we identify a novel fourth category of ChIs that is quantitatively and qualitatively distinct from the other three. This fourth group, which we have named mixed mode, has canonical tonic firing properties like regular ChIs with intermittent bursting-like rhythmic activity overlaid onto the regular pacemaker like firing patterns. We further characterized the effect of CRF on the four types of ChI firing patterns and discovered differential sensitivity to CRF, with irregular ChIs potentiating their firing at a lower concentration compared to the other groups along with a marked reduction in the IEI CV. A key insight of this study is that CRF shifts the ChI firing pattern distribution toward more regular firing. Finally, we show for the first time that sex and estrous cycle impact the ChI firing rate and distribution of ChI firing patterns. This work is among the first characterizing the firing modes of ChIs in the NAc shell, which may greatly add to our understanding of how these interneurons function on a fundamental level.

Based on previous literature and our own work, these spontaneous firing patterns are intrinsic to the cell as they cannot be altered by blockade of glutamatergic or GABAergic synaptic transmission (Bennett and Wilson, 1999). The difference in firing properties may be due in part to differences in SK expression or function since work from the Wilson lab showed that application of the SK antagonist apamin can shift ChI firing from a regular firing pattern to rhythmic bursting firing pattern (Bennett, Callaway and Wilson, 2000; Goldberg and Wilson, 2005; Wilson, 2005). Importantly, Bennett and Wilson (1999) demonstrated that these same spontaneous firing patterns are apparent in the intact animal using extracellular recordings, suggesting that differences in firing motifs may impact behavioral function (Bennett and Wilson, 1999). Without having access to the original data, it is challenging to know for certain why Bennett and Wilson (1999) did not detect the mixed mode ChI type. Based on their reports and our previous work, ChIs recorded in the dorsal striatum tend to have lower firing rates than ChIs in the NAc core or shell (Bennett and Wilson, 1999; Lemos, Shin and Alvarez, 2019), which perhaps makes it more difficult to distinguish irregular and mixed mode ChIs. It is also possible that NAc shell ChIs have a different composition of ion channels or SK

subtypes within the sK channel family that lead to the emergence of this fourth ChI type. A potential future direction could entail utilizing a method such as PatchSeq to connect ion channel composition and expression for each cell to their firing pattern.

Plasticity in ChI firing pattern driven by sex and estrous cycle

Here we found that NAc shell ChI firing rates and firing patterns differ between male and female mice. While this difference in ChIs is novel, sex differences in the firing rate of other tonically active neurons such as dopamine neurons have been observed, though the mechanism remains elusive (Calipari et al., 2017). Fascinatingly, in dopamine neurons, the direction is reversed such that females have higher firing rates compared to males. It is interesting that the proportion of ChI firing patterns shift across the estrous cycle as does the variance in firing rate. This finding indicates to us that there is state-dependent plasticity in spontaneous firing patterns in NAc shell ChIs. Differences in firing properties across the estrous cycle have also been observed in a number of cell types within the mesocorticolimbic pathway. Again, estrous-cycle driven changes have also been observed in dopamine neuron firing properties (Calipari et al., 2017; Shanley et al., 2023). Furthermore, in the cortex, there is a pronounced difference in the firing rate and firing pattern of FSIs recorded in awake behaving non-estrus and estrus females. Critically, the change in firing rate in response to social touch is only observed in non-estrus females, perhaps because the already elevated firing rate of FSIs found in estrus females occludes further elevation (Clemens et al., 2019). In the NAc, there are conflicting reports as to whether there are basal sex and estrous cycle differences in firing properties or synaptic transmission in medium spiny projection neurons, the main output neuron of the NAc. These conflicting findings may be due to differences in species, subregions, and internal states of the animal (Chapp, 2023; Proano et al., 2018; Willett et al., 2016). Nevertheless, we have identified a novel avenue through which estrous cycle can impact the circuit function of the NAc shell.

Neuromodulation and plasticity of ion channel function

CRF exerts its actions on cell excitability via SK channel enhancement in both ChIs and dopamine neurons(Lemos, Shin and Alvarez, 2019; Riegel and Williams, 2008); in ChIs it does so by reducing spike accommodation. High SK channel activation gives rise to

the medium-duration afterhyperpolarization potential (mAHP), which allows for regular single spiking activity, while low SK channel activity is necessary for bursting(Goldberg and Wilson, 2005). Based on both Lemos et al., (2019) and Goldberg and Wilson (2015) one could conclude that CRF increases SK channel activity in rhythmic bursting and irregular cell types to promote pacemaker activity and prevent bursting activity. High baseline SK activation in regular spiking neurons could occlude CRF effects, particularly at lower concentrations, because they are already highly active. Though we did not find any studies assessing change in SK activation across estrous cycle, there have been reports of changes in the function of other potassium channels across estrous cycle. In both GnRH neurons of the medial preoptic area and CRF neurons within the paraventricular nucleus of the hypothalamus, I_A channel conductance is elevated during estrus and diestrus compared to proestrus(Arroyo et al., 2011; Power and Iremonger, 2021). Regulation of potassium channel conductances may be a conserved mechanism in which ovarian hormonal cycle can induce transient changes in the excitability of several cell types across the brain.

Implications for accumbal microcircuitry

The nucleus accumbens is composed of important microdomains or functional units that can control different circuit outputs and behavioral repertoires (Brimblecombe and Cragg, 2017; Burke, Rotstein and Alvarez, 2017; Gangarossa et al., 2013a; Gangarossa et al., 2013b; Gangarossa, Perroy and Valjent, 2013). The level of granularity of these microdomains and what truly defines them remains an active area of study. For example, an open question is whether these domains are driven by lateral connectivity between MSNs, excitatory projections into individual subregions, or the target projections of each subregion. Within the nucleus accumbens core and shell there are hotspots of both cholinergic activity and the function of other neuromodulators such as dopamine.

The spontaneous activity of cholinergic interneurons ensures an ambient level of acetylcholine, which can in turn bind nicotinic and muscarinic receptors. Focusing on muscarinic receptors, all five cloned receptors are present in the striatum, either on striatal neurons themselves or cortical and/or dopamine terminals (Benarroch, 2012;

Razidlo et al., 2022). How and when these receptors are differentially or cooperatively activated in the intact circuit is poorly understood. However, it is possible that different firing motifs of ChIs may bias toward activation of one subtype over another.

The synchronous optogenetic activation of cholinergic interneurons in the nucleus accumbens can trigger dopamine and glutamate release from dopaminergic varicosities via activation of β2-containing nicotinic acetylcholine receptors (Adrover, Shin and Alvarez, 2014; Cachope and Cheer, 2014; Cachope et al., 2012; Rice and Cragg, 2004; Threlfell et al., 2012). Indeed, activation of nAChRs on dopamine varicosities is sufficient to trigger action potentials within the *en passante* boutons (Kramer et al., 2022; Liu et al., 2022). Recent work has demonstrated that spontaneous dopamine transients detected in the ex vivo slice preparation are driven by the spontaneous activity of cholinergic interneurons (Yorgason, Zeppenfeld and Williams, 2017). It is possible that different firing motifs, for example, rhythmic or mixed mode with burst-like activity might differentially promote the spontaneous dopamine transients more than regular or irregular firing patterns.

One notion that we have not addressed in this manuscript is the fact that cholinergic interneurons form small clusters throughout the striatum (Carrasco et al., 2022; Gangarossa et al., 2013b). The functional significance of these clusters has not been studied at the circuit or behavioral levels. However, we do know that ChIs within the clusters are functionally coupled compared to ChIs within adjacent clusters. In other words, changes in activity in one ChI within a cluster can influence the activity of the other ChIs in the cluster via GABAergic interneurons (Dorst et al., 2020). One remaining question is how spontaneous ChI firing motifs and shifts in firing motifs alter the function of the individual ChI clusters. Utilizing novel genetically encoded voltage sensors within the *ex vivo* preparation would give us important insights into these interactions.

Implications for circuit function and behavior

At a cellular level, it has been suggested that burst-pause motifs allow for windows in which plasticity can occur (Ding et al., 2010). At the behavioral level, shifts in cholinergic interneuron firing motifs from pacemaker to burst-pause and back to pacemaker can encode salient environmental cues such as changes in contingency, cues that signal

reward and novelty (Aoki et al., 2018; Aoki et al., 2015; Bradfield and Balleine, 2017; Ding et al., 2010; Dorst et al., 2020; Mohebi, Collins and Berke, 2023; Zhang and Cragg, 2017; Zucca et al., 2018). The mechanisms driving changes in firing motifs remain controversial. The preponderance of the literature indicates that these burst-pause events are driven by a combination of glutamatergic inputs and intrinsic ChI properties and are reliant on activation of dopamine D2 receptors localized to ChIs (Chantranupong et al., 2023; Chuhma et al., 2014; Ding et al., 2010; Zhang and Cragg, 2017; Zucca et al., 2018). We propose that the composition of ChI firing motifs differentially poises the cells to respond to different inputs and neuromodulators.

CRF is a stress-associated neuromodulator that is released in response to salient stimuli (Merali, McIntosh and Anisman, 2004; Wang et al., 2005). In the nucleus accumbens, endogenous CRF is released in response to novelty and serves to promote engagement with the environment (Lemos et al., 2012). In this study we demonstrated that ChIs with different spontaneous firing properties are differentially sensitive to CRF. Irregular firing ChIs show changes in both firing rate and CV at low, mid, and high exogenously applied concentrations of CRF. The CRF response (percent of baseline firing) is negatively correlated with the baseline firing rate. This relationship between baseline firing and CRF response may explain the increased sensitivity of irregular ChIs to CRF. Thus, as a population, differences in ChI firing pattern modes would potentially determine how the circuit responds to CRF evoked by salient stimuli. While this would matter less with highly salient stimuli that presumably evoked more CRF, it would come into play with stimuli that had mild or modest salience, such as novel objects that may evoke some CRF but at lower overall concentrations. This notion has been shown via proxy measurements of release using fiber photometry in the paraventricular nucleus of hypothalamus and cortex (Kim et al., 2019; Wang, 2022). This speculation highlights a missing link in our understanding of neuropeptide signaling. It remains technologically intractable to measure absolute concentrations of neuropeptide release (as opposed to percent change in baseline) in awake behaving animals. Thus, it is difficult to test the hypothesis that stimuli with different valence or salience evoke different concentrations of CRF in the NAc or any other region or relate these measures back to the exogenous application of CRF applied to the slice. A central discovery of this study is that CRF

alters the proportion of ChI spontaneous firing patterns toward more regular pacemaker activity. While consequences of this shift are not clear, it could allow salient, even stressful, stimuli to shift the network activity of the NAc to alter motivated behavior. In the future, we hope to measure both CRF and ChI activity simultaneously in the behaving animal, including male and female animals across the estrous cycle, and determine whether stimuli with different salience differentially evokes increases in CRF and cholinergic activity.

Limitations

Rhythmic bursting cells were sparse in number and were also more challenging to hold at a gigaohm seal through the experiment. This made it challenging to accumulate robust sample sizes for all concentrations of CRF. Thus, we had a significant amount of variability at lower CRF concentrations. Likewise, it was very difficult to capture females in the proestrus and metestrus phases of the estrous cycle since those stages are much shorter than diestrus and estrus. As such, our sample sizes are smaller for those cycle stages. However, considering the difference in the proportion of ChI firing patterns across all four stages, we felt it was important not to pool data into high and low estradiol groups, for example. We can only speculate about what these cellular observations mean for the behaving animal. However, we hope that these ex vivo findings will trigger a new set of testable hypotheses for in vivo studies.

References

1. Adrover, M.F., Shin, J.H., Alvarez, V.A., 2014. Glutamate and dopamine transmission from midbrain dopamine neurons share similar release properties but are differentially affected by cocaine. J Neurosci 34, 3183-3192.
2. Al-Hasani, R., Gowrishankar, R., Schmitz, G.P., Pedersen, C.E., Marcus, D.J., Shirley, S.E., Hobbs, T.E., Elerding, A.J., Renaud, S.J., Jing, M., Li, Y., Alvarez, V.A., Lemos, J.C., Bruchas, M.R., 2021. Ventral tegmental area GABAergic inhibition of cholinergic interneurons in the ventral nucleus accumbens shell promotes reward reinforcement. Nat Neurosci 24, 1414-1428.
3. Aoki, S., Liu, A.W., Akamine, Y., Zucca, A., Zucca, S., Wickens, J.R., 2018. Cholinergic interneurons in the rat striatum modulate substitution of habits. Eur J Neurosci 47, 1194-1205.

4. Aoki, S., Liu, A.W., Zucca, A., Zucca, S., Wickens, J.R., 2015. Role of Striatal Cholinergic Interneurons in Set-Shifting in the Rat. J Neurosci 35, 9424-9431.
5. Arroyo, A., Kim, B.S., Biehl, A., Yeh, J., Bett, G.C., 2011. Expression of kv4.3 voltage-gated potassium channels in rat gonadotrophin-releasing hormone (GnRH) neurons during the estrous cycle. Reprod Sci 18, 136-144.
6. Bale, T.L., Vale, W.W., 2004. CRF and CRF receptors: role in stress responsivity and other behaviors. Annual review of pharmacology and toxicology 44, 525-557.
7. Benarroch, E.E., 2012. Effects of acetylcholine in the striatum. Recent insights and therapeutic implications. Neurology 79, 274-281.
8. Bennett, B.D., Callaway, J.C., Wilson, C.J., 2000. Intrinsic membrane properties underlying spontaneous tonic firing in neostriatal cholinergic interneurons. J Neurosci 20, 8493-8503.
9. Bennett, B.D., Wilson, C.J., 1999. Spontaneous activity of neostriatal cholinergic interneurons in vitro. J Neurosci 19, 5586-5596.
10. Bolam, J.P., Wainer, B.H., Smith, A.D., 1984. Characterization of cholinergic neurons in the rat neostriatum. A combination of choline acetyltransferase immunocytochemistry, Golgi-impregnation and electron microscopy. Neuroscience 12, 711-718.
11. Bonsi, P., Cuomo, D., Martella, G., Madeo, G., Schirinzi, T., Puglisi, F., Ponterio, G., Pisani, A., 2011. Centrality of striatal cholinergic transmission in Basal Ganglia function. Front Neuroanat 5, 6.
12. Bradfield, L.A., Balleine, B.W., 2017. Thalamic Control of Dorsomedial Striatum Regulates Internal State to Guide Goal-Directed Action Selection. J Neurosci 37, 3721-3733.
13. Brimblecombe, K.R., Cragg, S.J., 2017. The Striosome and Matrix Compartments of the Striatum: A Path through the Labyrinth from Neurochemistry toward Function. ACS Chem Neurosci 8, 235-242.
14. Burke, D.A., Rotstein, H.G., Alvarez, V.A., 2017. Striatal Local Circuitry: A New Framework for Lateral Inhibition. Neuron 96, 267-284.
15. Cachope, R., Cheer, J.F., 2014. Local control of striatal dopamine release. Front Behav Neurosci 8, 188.
16. Cachope, R., Mateo, Y., Mathur, B.N., Irving, J., Wang, H.L., Morales, M., Lovinger, D.M., Cheer, J.F., 2012. Selective activation of cholinergic interneurons enhances accumbal phasic dopamine release: setting the tone for reward processing. Cell Rep 2, 33-41.
17. Calipari, E.S., Juarez, B., Morel, C., Walker, D.M., Cahill, M.E., Ribeiro, E., Roman-Ortiz, C., Ramakrishnan, C., Deisseroth, K., Han, M.H., Nestler, E.J., 2017. Dopaminergic dynamics underlying sex-specific cocaine reward. Nat Commun 8, 13877.
18. Carrasco, A., Oorschot, D.E., Barzaghi, P., Wickens, J.R., 2022. Three-Dimensional Spatial Analyses of Cholinergic Neuronal Distributions Across The Mouse Septum, Nucleus Basalis, Globus Pallidus, Nucleus Accumbens, and Caudate-Putamen. Neuroinformatics 20, 1121-1136.
19. Chantranupong, L., Beron, C.C., Zimmer, J.A., Wen, M.J., Wang, W., Sabatini, B.L., 2023. Dopamine and glutamate regulate striatal acetylcholine in decision-making. Nature.

20. Chapp, A.D., Nwakama, C.A., Jagtap, P.P., Phan, C.H., Thomas, M.J., Mermelstein, P.G., 2023. Fundamental Sex Differences in Cocaine-Induced Plasticity of D1- and D2-MSNs in the Mouse Nucleus Accumbens Shell. BioRIX.
21. Chen, Y.W., Rada, P.V., Butzler, B.P., Leibowitz, S.F., Hoebel, B.G., 2012. Corticotropin-releasing factor in the nucleus accumbens shell induces swim depression, anxiety, and anhedonia along with changes in local dopamine/acetylcholine balance. Neuroscience 206, 155-166.
22. Chuhma, N., Mingote, S., Moore, H., Rayport, S., 2014. Dopamine neurons control striatal cholinergic neurons via regionally heterogeneous dopamine and glutamate signaling. Neuron 81, 901-912.
23. Clemens, A.M., Lenschow, C., Beed, P., Li, L., Sammons, R., Naumann, R.K., Wang, H., Schmitz, D., Brecht, M., 2019. Estrus-Cycle Regulation of Cortical Inhibition. Curr Biol 29, 605-615 e606.
24. Cora, M.C., Kooistra, L., Travlos, G., 2015. Vaginal Cytology of the Laboratory Rat and Mouse: Review and Criteria for the Staging of the Estrous Cycle Using Stained Vaginal Smears. Toxicol Pathol 43, 776-793.
25. Dabrowska, J., Hazra, R., Guo, J.D., Dewitt, S., Rainnie, D.G., 2013. Central CRF neurons are not created equal: phenotypic differences in CRF-containing neurons of the rat paraventricular hypothalamus and the bed nucleus of the stria terminalis. Front Neurosci 7, 156.
26. Ding, J.B., Guzman, J.N., Peterson, J.D., Goldberg, J.A., Surmeier, D.J., 2010. Thalamic gating of corticostriatal signaling by cholinergic interneurons. Neuron 67, 294-307.
27. Dorst, M.C., Tokarska, A., Zhou, M., Lee, K., Stagkourakis, S., Broberger, C., Masmanidis, S., Silberberg, G., 2020. Polysynaptic inhibition between striatal cholinergic interneurons shapes their network activity patterns in a dopamine-dependent manner. Nat Commun 11, 5113.
28. Gangarossa, G., Espallergues, J., de Kerchove d'Exaerde, A., El Mestikawy, S., Gerfen, C.R., Herve, D., Girault, J.A., Valjent, E., 2013a. Distribution and compartmental organization of GABAergic medium-sized spiny neurons in the mouse nucleus accumbens. Front Neural Circuits 7, 22.
29. Gangarossa, G., Espallergues, J., Mailly, P., De Bundel, D., de Kerchove d'Exaerde, A., Herve, D., Girault, J.A., Valjent, E., Krieger, P., 2013b. Spatial distribution of D1R- and D2R-expressing medium-sized spiny neurons differs along the rostro-caudal axis of the mouse dorsal striatum. Front Neural Circuits 7, 124.
30. Gangarossa, G., Perroy, J., Valjent, E., 2013. Combinatorial topography and cell-type specific regulation of the ERK pathway by dopaminergic agonists in the mouse striatum. Brain Struct Funct 218, 405-419.
31. Goldberg, J.A., Wilson, C.J., 2005. Control of spontaneous firing patterns by the selective coupling of calcium currents to calcium-activated potassium currents in striatal cholinergic interneurons. J Neurosci 25, 10230-10238.
32. Gonzales, K.K., Smith, Y., 2015. Cholinergic interneurons in the dorsal and ventral striatum: anatomical and functional considerations in normal and diseased conditions. Ann N Y Acad Sci 1349, 1-45.

33. Henckens, M.J., Deussing, J.M., Chen, A., 2016. Region-specific roles of the corticotropin-releasing factor-urocortin system in stress. Nat Rev Neurosci 17, 636-651.
34. Kim, J., Lee, S., Fang, Y.Y., Shin, A., Park, S., Hashikawa, K., Bhat, S., Kim, D., Sohn, J.W., Lin, D., Suh, G.S.B., 2019. Rapid, biphasic CRF neuronal responses encode positive and negative valence. Nat Neurosci 22, 576-585.
35. Kramer, P.F., Brill-Weil, S.G., Cummins, A.C., Zhang, R., Camacho-Hernandez, G.A., Newman, A.H., Eldridge, M.A.G., Averbeck, B.B., Khaliq, Z.M., 2022. Synaptic-like axo-axonal transmission from striatal cholinergic interneurons onto dopaminergic fibers. Neuron 110, 2949-2960 e2944.
36. Krok, A.C., Maltese, M., Mistry, P., Miao, X., Li, Y., Tritsch, N.X., 2023. Intrinsic dopamine and acetylcholine dynamics in the striatum of mice. Nature.
37. Lemos, J.C., Shin, J.H., Alvarez, V.A., 2019. Striatal cholinergic interneurons are a novel target of corticotropin releasing factor. J Neurosci.
38. Lemos, J.C., Wanat, M.J., Smith, J.S., Reyes, B.A., Hollon, N.G., Van Bockstaele, E.J., Chavkin, C., Phillips, P.E., 2012. Severe stress switches CRF action in the nucleus accumbens from appetitive to aversive. Nature 490, 402-406.
39. Lim, M.M., Liu, Y., Ryabinin, A.E., Bai, Y., Wang, Z., Young, L.J., 2007. CRF receptors in the nucleus accumbens modulate partner preference in prairie voles. Hormones and behavior 51, 508-515.
40. Liu, C., Cai, X., Ritzau-Jost, A., Kramer, P.F., Li, Y., Khaliq, Z.M., Hallermann, S., Kaeser, P.S., 2022. An action potential initiation mechanism in distal axons for the control of dopamine release. Science 375, 1378-1385.
41. Merali, Z., McIntosh, J., Anisman, H., 2004. Anticipatory cues differentially provoke in vivo peptidergic and monoaminergic release at the medial prefrontal cortex. Neuropsychopharmacology 29, 1409-1418.
42. Mohebi, A., Collins, V.L., Berke, J.D., 2023. Accumbens cholinergic interneurons dynamically promote dopamine release and enable motivation. Elife 12.
43. Nosaka, D., Wickens, J.R., 2022. Striatal Cholinergic Signaling in Time and Space. Molecules 27.
44. Pecina, S., Schulkin, J., Berridge, K.C., 2006. Nucleus accumbens corticotropin-releasing factor increases cue-triggered motivation for sucrose reward: paradoxical positive incentive effects in stress? BMC biology 4, 8.
45. Power, E.M., Iremonger, K.J., 2021. Plasticity of intrinsic excitability across the estrous cycle in hypothalamic CRH neurons. Sci Rep 11, 16700.
46. Proano, S.B., Morris, H.J., Kunz, L.M., Dorris, D.M., Meitzen, J., 2018. Estrous cycle-induced sex differences in medium spiny neuron excitatory synaptic transmission and intrinsic excitability in adult rat nucleus accumbens core. J Neurophysiol 120, 1356-1373.
47. Razidlo, J.A., Fausner, S.M.L., Ingebretson, A.E., Wang, L.C., Petersen, C.M., Mirza, S., Swank, I.N., Alvarez, V.A., Lemos, J.C., 2022. Chronic loss of muscarinic M5 receptor function manifests disparate impairments in exploratory behavior in male and female mice despite common dopamine regulation. J Neurosci 42, 6917-6930.

48. Rice, M.E., Cragg, S.J., 2004. Nicotine amplifies reward-related dopamine signals in striatum. Nat Neurosci 7, 583-584.
49. Riegel, A.C., Williams, J.T., 2008. CRF facilitates calcium release from intracellular stores in midbrain dopamine neurons. Neuron 57, 559-570.
50. Shanley, M.R., Miura, Y., Guevara, C.A., Onoichenco, A., Kore, R., Ustundag, E., Darwish, R., Renzoni, L., Urbaez, A., Blicker, E., Seidenberg, A., Milner, T.A., Friedman, A.K., 2023. Estrous Cycle Mediates Midbrain Neuron Excitability Altering Social Behavior upon Stress. J Neurosci 43, 736-748.
51. Threlfell, S., Lalic, T., Platt, N.J., Jennings, K.A., Deisseroth, K., Cragg, S.J., 2012. Striatal dopamine release is triggered by synchronized activity in cholinergic interneurons. Neuron 75, 58-64.
52. Wang, B., Shaham, Y., Zitzman, D., Azari, S., Wise, R.A., You, Z.B., 2005. Cocaine experience establishes control of midbrain glutamate and dopamine by corticotropin-releasing factor: a role in stress-induced relapse to drug seeking. J Neurosci 25, 5389-5396.
53. Wang, H., Qian, T., Zhao, Y., Zhuo, Y., Wu, C., Osakada, T., Chen, P., Ren, H., Yan, Y., Geng, L., Fu, S., Mei, L., Li, G., Wu,L., Jiang,Y., Qian, W., Peng, W., Xu, M.,Hu, J., Chen, L.,Tang,C. Lin, D.Zhou,J.N., Yulong Li,Y., 2022. A toolkit of highly selective and sensitive genetically encoded 1 neuropeptide sensors BioRIX.
54. Willett, J.A., Will, T., Hauser, C.A., Dorris, D.M., Cao, J., Meitzen, J., 2016. No Evidence for Sex Differences in the Electrophysiological Properties and Excitatory Synaptic Input onto Nucleus Accumbens Shell Medium Spiny Neurons. eNeuro 3.
55. Wilson, C.J., 2005. The mechanism of intrinsic amplification of hyperpolarizations and spontaneous bursting in striatal cholinergic interneurons. Neuron 45, 575-585.
56. Yorgason, J.T., Zeppenfeld, D.M., Williams, J.T., 2017. Cholinergic Interneurons Underlie Spontaneous Dopamine Release in Nucleus Accumbens. J Neurosci 37, 2086-2096.
57. Zhang, Y.F., Cragg, S.J., 2017. Pauses in Striatal Cholinergic Interneurons: What is Revealed by Their Common Themes and Variations? Front Syst Neurosci 11, 80.
58. Zucca, S., Zucca, A., Nakano, T., Aoki, S., Wickens, J., 2018. Pauses in cholinergic interneuron firing exert an inhibitory control on striatal output in vivo. Elife 7.

Figure Legends

Figure 1. Cholinergic interneurons (ChIs) in the NAc shell have four distinct firing modes. A) Example traces of cell-attached recordings and B) corresponding frequency histograms of the inter-event interval made from regular, rhythmic, irregular and mixed mode ChIs recorded in the NAc shell. C) Pie chart of distribution of ChI spontaneous firing pattern from 108 cells recorded in NAc shell of male and female mice. D) Summary data of firing rates for regular, rhythmic, irregular and mixed mode ChIs. Tukey's post-hoc t-tests were used following a one-way ANOVA: Regular vs. Rhythmic, $p = 0.0031$, Regular vs. Irregular, $p < 0.0001$, Irregular vs. Mixed Mode, $p = 0.0019$. All other comparisons were not significant. E) Summary data of CV for IEI for regular, rhythmic, irregular and mixed mode ChIs. Dunn's post-hoc t-tests were used following a Kruskal-Wallis test: Regular vs. Rhythmic; vs. Irregular; vs. Mixed Mode, ps < 0.0001, Regular vs. Irregular vs. Rhythmic, $p = 0.0028$, Irregular vs. Mixed Mode, $p = 0.0025$. All other comparisons were not significant. F) Firing rate x CV plot for 108 ChIs recorded in NAc shell. ChIs are color coded based on firing mode (regular = magenta, rhythmic = grey, irregular = light blue, mixed mode = purple). There was significant negative correlation between firing rate and CV, $r^2 = -0.464$, $p < 0.0001$.

Figure 2. Sex differences in NAc shell ChI firing properties. A) Example traces of cell-attached recordings made from NAc shell ChIs in male (top) and female (bottom) mice. B) Summary data of firing rates recorded in male and female mice. Mann-Whitney test, ** $p = 0.0024$. C) Summary data of CV of IEI for ChIs recorded in male and female mice. E) Example images of vaginal cytology used to classify females into proestrus, estrus, metestrus and diestrus cycle stages. E) Summary data of firing rates recorded in NAc shell ChI from male and female mice across the estrous cycle. Dunn's post-hoc t-tests were used following a Kruskal-Wallis test: Male vs. Estrus, $p = 0.0169$; Male vs. Diestrus, $p = 0.0143$. F) Summary data of CV of IEI recorded in NAc shell ChI from male and female mice across the estrous cycle. G) Distribution of ChI firing mode in male and females (pooled, left) across estrous cycle (separated, right). Chi-squared test of male vs. female, p 0.0260; Chi-squared test of female across estrous cycle, $p < 0.001$.

Figure 3. Blockade of glutamatergic synaptic transmission does not shift ChI firing properties. A) Pie chart of distribution of ChI spontaneous firing pattern from 14 recorded in NAc shell of male and female mice in the presence of NBQX and CPP. B) Summary data of firing rates for ChIs recorded in control ACSF (108) and ChIs recorded in the presence of NBQX and CPP (14). C) Summary data of CV of IEI for ChIs recorded in control ACSF (108) and ChIs recorded in the presence of NBQX and CPP (14). E) Firing rate x CV plot for 14 ChIs recorded in NAc shell in the presence of NBQX and CPP. ChIs are color coded based on firing mode (regular = magenta, rhythmic = grey, irregular = light blue, mixed mode = purple). There was a negative correlation between firing rate and CV, r^2 = -0.463 that trended toward significance, p = 0.096.

Figure 4. Differential sensitivity to CRF based on ChI firing mode. A) Example trace of cell-attached recordings prior to and following CRF in from a Regular ChI. B) Summary data of CRF effect on firing rate (% baseline) for 0, 3, 10, 100 nM in Regular ChIs. ** = One-sample t-test of CRF (10 nM) effect (% baseline) vs 100, p = 0.0029; ** = One-sample t-test of CRF (100 nM) effect (% baseline) vs 100, p = 0.0079. C) Summary data of CRF effect on CV of IEI (ΔCV) for 0, 3, 10, 100 nM in Regular ChIs. D) Change in ChI firing pattern distribution following application of CRF (0,3,10, 100 nM) in Regular ChIs. E) Example trace of cell-attached recordings prior to and following CRF in from a Rhythmic ChI. F) Summary data of CRF effect on firing rate (% baseline) for 0, 3, 10, 100 nM in Rhytmic ChIs. * = One-sample t-test of CRF (100 nM) effect (% baseline) vs 100, p = 0.0314. G) Summary data of CRF effect on CV of IEI (ΔCV) for 0, 3, 10, 100 nM in Rhythmic ChIs. H) Change in ChI firing pattern distribution following application of CRF (0,3,10, 100 nM) in Rhythmic ChIs. I) Example trace of cell-attached recordings prior to and following CRF in from a Irregular ChI. J) Summary data of CRF effect on firing rate (% baseline) for 0, 3, 10, 100 nM in Irregular ChIs. ** = One-sample t-test of CRF (3 nM) effect (% baseline) vs 100, p = 0.0038; *** = One-sample t-test of CRF (10 nM) effect (% baseline) vs 100, p = 0.0004; *** = One-sample t-test of CRF (100 nM) effect (% baseline) vs 100, p = 0.0002. K) Summary data of CRF effect on CV of IEI

(ΔCV) for 0, 3, 10, 100 nM in Irregular ChIs. * = One-sample t-test of CRF (10 nM) effect (ΔCV) vs 0, p = 0.0350; *** = One-sample t-test of CRF (100 nM) effect (ΔCV) vs 0, p = 0.0009. L) Change in ChI firing pattern distribution following application of CRF (0,3,10, 100 nM) in Irregular ChIs. M) Example trace of cell-attached recordings prior to and following CRF in from a Mixed Mode ChI. N) Summary data of CRF effect on firing rate (% baseline) for 0, 3, 10, 100 nM in Mixed Mode ChIs. * = One-sample t-test of CRF (10 nM) effect (% baseline) vs 100, p = 0.0124; **= One-sample t-test of CRF (100 nM) effect (% baseline) vs 100, p = 0.0074. O) Summary data of CRF effect on CV of IEI (ΔCV) for 0, 3, 10, 100 nM in Mixed Mode ChIs. P) Change in ChI firing pattern distribution following application of CRF (0,3,10, 100 nM) in Mixed Mode ChIs.

Figure 5. CRF shifts ChI firing properties toward a regular firing pattern. A) Summary data of CRF (3 nM) effect on firing rate (% baseline) for regular, rhythmic, irregular and mixed mode ChIs.* = Tukey's post-hoc t-test, p = 0.0468. B) Summary data of CRF (100 nM) effect on firing rate (% baseline) for regular, rhythmic, irregular and mixed mode ChIs. C) CRF 100 nM response (%baseline) x baseline firing rate plot for 39 ChIs recorded in NAc shell prior to and following CRF. ChIs are color coded based on firing mode (regular = magenta, rhythmic = grey, irregular = light blue, mixed mode = purple). Data is fit with a semi-log line, $r^2 = -0.60$, $p < 0.001$. D) Firing pattern distribution in ChIs prior to (left) and following (right) CRF (100 nM) bath application.

Author Contributions: AEI and JCL conceived and designed research. AEI and JCL performed experiments, analyzed data, and interpreted results of experiments. AEI and JCL prepared figures, drafted manuscript, edited and revised manuscript. AEI and JCL approved the final version of manuscript.

Figure 1. Cholinergic interneurons (ChIs) in the NAc shell have four distinct firing modes

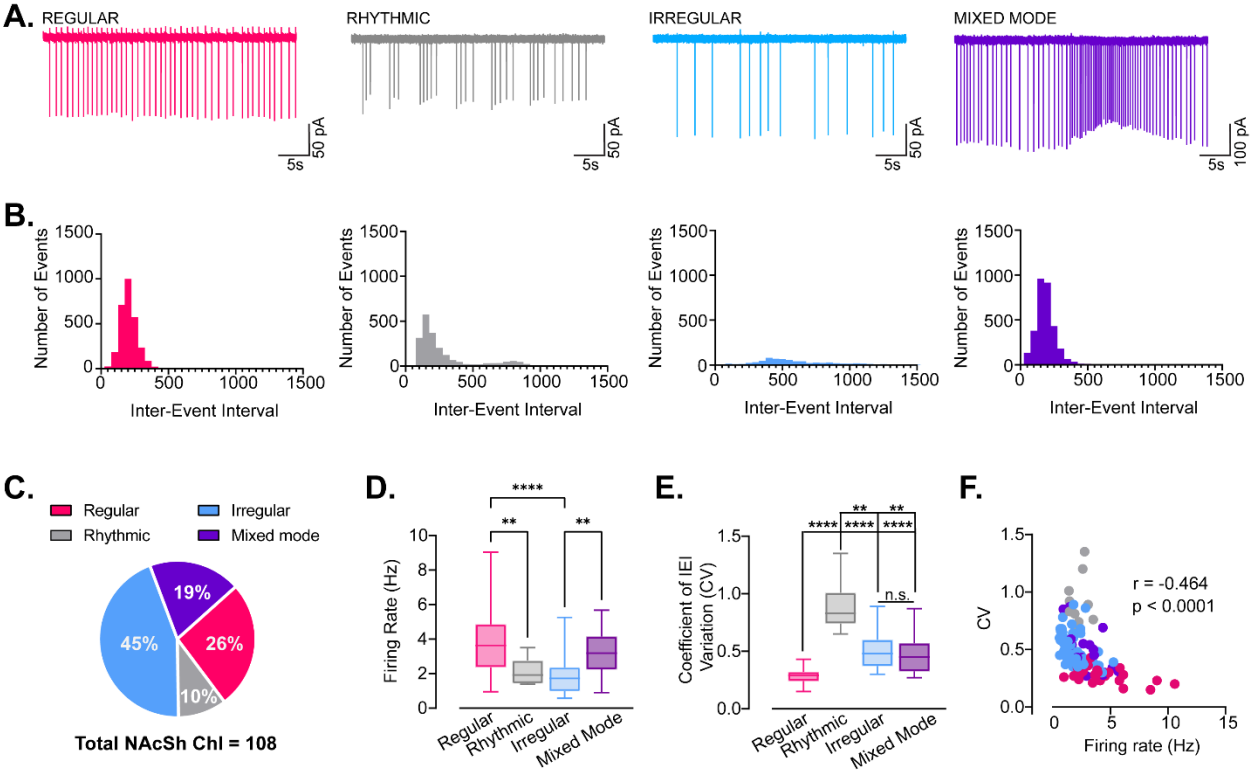

Figure 2. Sex differences in NAc shell ChI firing properties

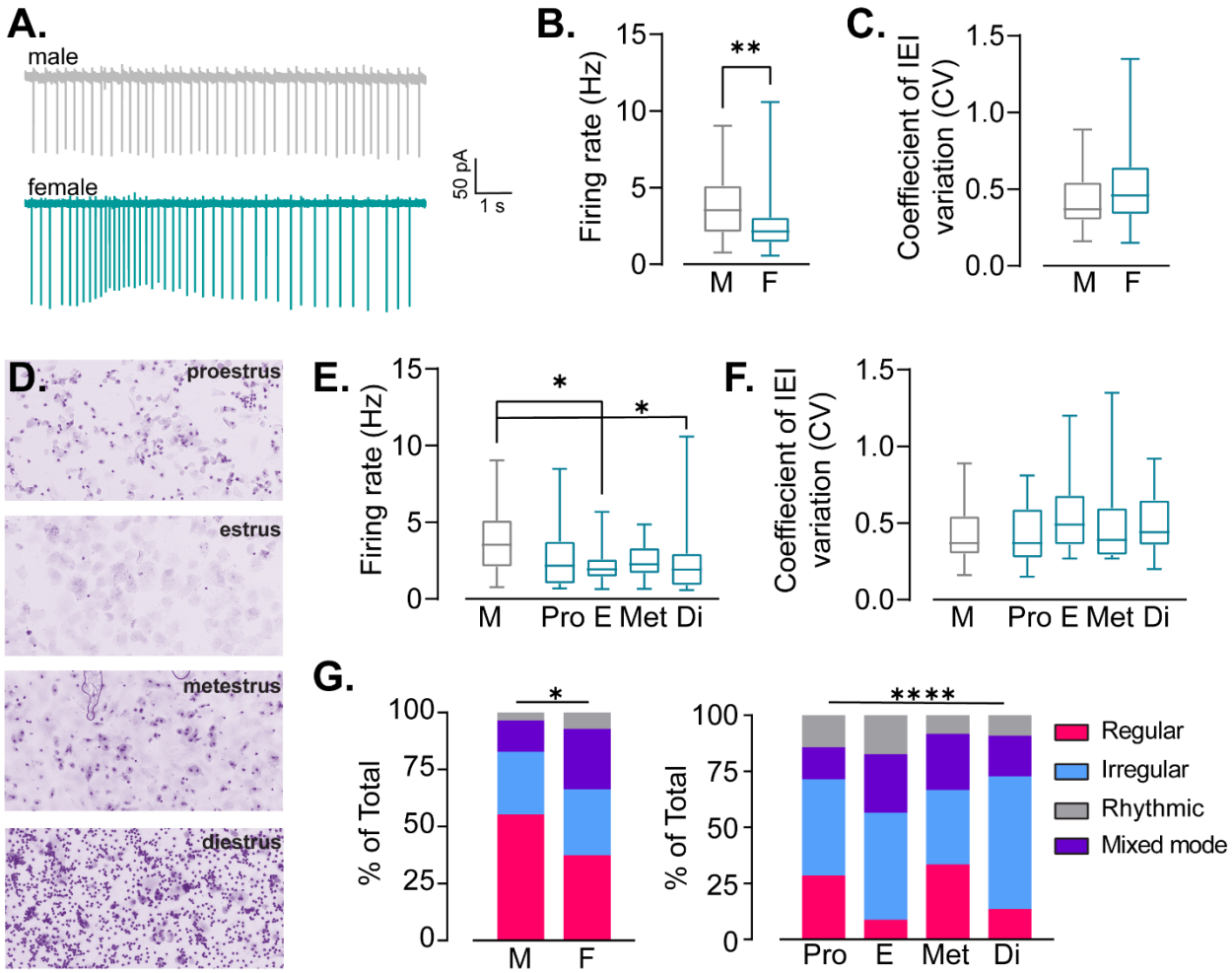

Figure 3. Blockade of glutamatergic synaptic transmission does not shift ChI firing properties

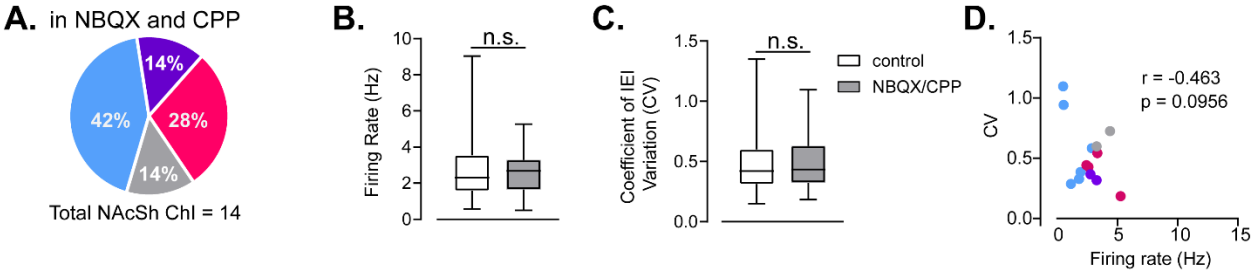

Figure 4. Differential sensitivity to CRF based on firing mode

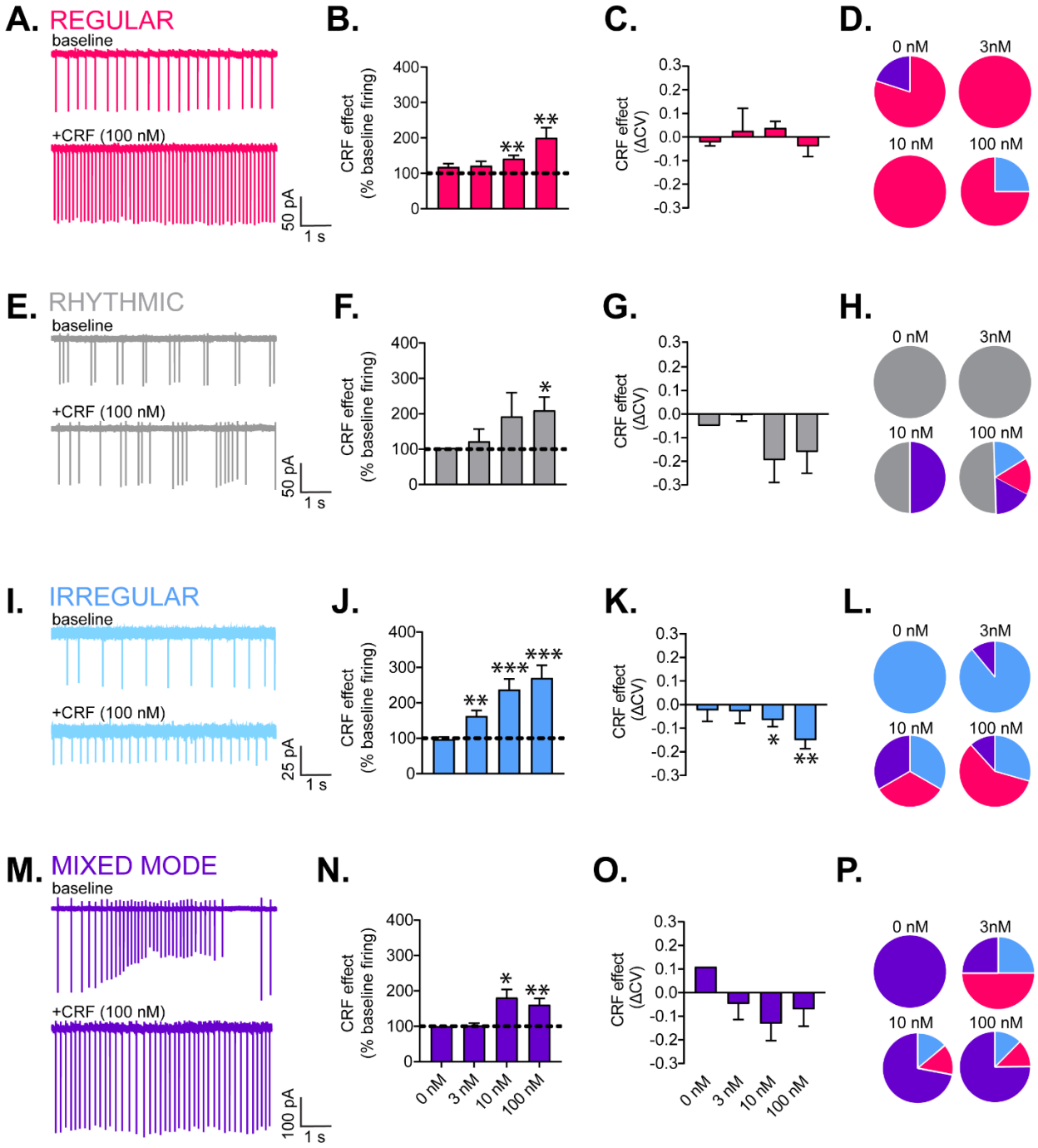
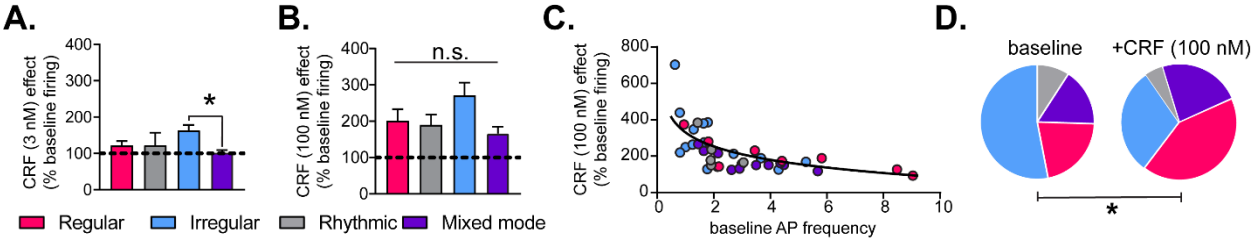
Figure 5. CRF shifts ChI firing properties toward regular firing pattern